

---

# PrObE D: Proactive Object Detection Wrapper

---

**Vishal Asnani**  
Michigan State University  
asnani@msu.edu

**Abhinav Kumar**  
Michigan State University  
kumarab6@msu.edu

**Suya You**  
DEVCOM Army Research Laboratory  
suya.you.civ@army.mil

**Xiaoming Liu**  
Michigan State University  
liuxm@cse.msu.edu

## Abstract

Previous research in  $2D$  object detection focuses on various tasks, including detecting objects in generic and camouflaged images. These works are regarded as passive works for object detection as they take the input image as is. However, convergence to global minima is not guaranteed to be optimal in neural networks; therefore, we argue that the trained weights in the object detector are not optimal. To rectify this problem, we propose a wrapper based on proactive schemes, PrObE D, which enhances the performance of these object detectors by learning a signal. PrObE D consists of an encoder-decoder architecture, where the encoder network generates an image-dependent signal termed templates to encrypt the input images, and the decoder recovers this template from the encrypted images. We propose that learning the optimum template results in an object detector with an improved detection performance. The template acts as a mask to the input images to highlight semantics useful for the object detector. Finetuning the object detector with these encrypted images enhances the detection performance for both generic and camouflaged. Our experiments on MS-COCO, CAMO, COD10K, and NC4K datasets show improvement over different detectors after applying PrObE D. Our models/codes are available at <https://github.com/vishal3477/Proactive-Object-Detection>.

## 1 Introduction

Generic  $2D$  object detection (GOD) has improved from earlier traditional detectors [15, 20, 64, 65] to the deep-learning-based object detectors [8, 10, 26, 32, 52, 58]. Advancements in deep-learning-based methods underwent many architectural change over recent years, including one-stage [5, 43, 46, 52–54], two-stage [23, 24, 58], CNN-based [5, 14, 16, 21–23, 52, 54], transformer-based [8, 74], and diffusion-based [10] methods. All these methods aim to predict the  $2D$  bounding box of the objects in the images and their category class.

Another emerging area related to generic object detection is camouflaged object detection [17, 18, 27–29, 34, 40] (COD). COD aims to detect and segment objects blended with the background [17, 18] via object-level mask supervision. Applications of COD include medical [19, 45], surveillance [11] and autonomous driving [69]. Early COD detectors exploit hand-crafted features [50, 61] and optical flow [33], while current methods are deep-learning-based. These methods utilize attention [9, 63], joint learning [40], image gradient [34], and transformers [48, 70].

All these methods take input images as is for the detection task and hence are called passive methods. However, there is a line of research on proactive methods for a wide range of vision tasks such as disruption [59, 60], tagging [68], manipulation detection [1], and localization [2]. Proactive methods

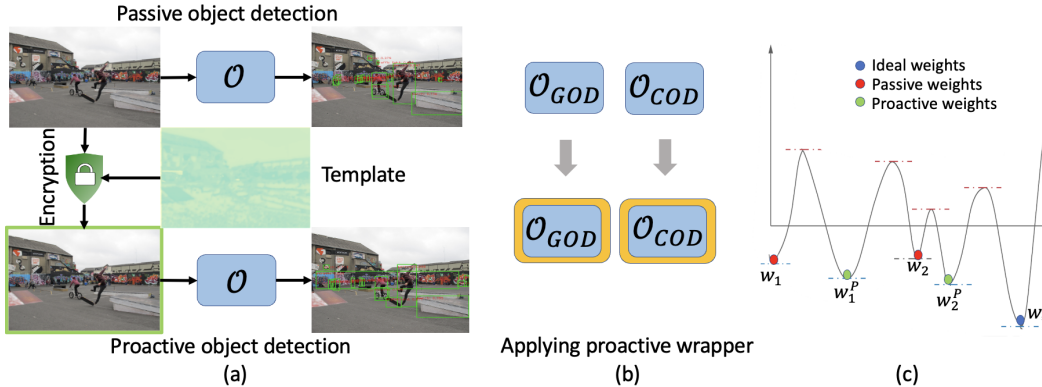


**Figure 1: (a) Passive vs. Proactive object detection.** A learnable template encrypts the input images, which are further used to train the object detector. **(b) PrObE D** serves as a wrapper on both generic and camouflaged object detectors, enhancing the detection performance. **(c)** For the linear regression model under additive noise and other assumptions, the converged weights of the proactive detector are closer to the optimal weights as compared to the converged weights of the passive detector. See Sec. 3.2 for details and proof.

use signals, called templates, to encrypt the input images and pass the encrypted images as the input to the network. These are trained in an end-to-end manner by using either a fixed [68] or learnable template [1, 2, 59, 60] to improve the performance. A major advantage of proactive schemes is that such methods generalize better on unseen data/models [1, 2]. Motivated by this, we propose a plug-and-play Proactive Object Detection wrapper, PrObE D, to improve GOD and COD detectors.

Designing PrObE D as a proactive scheme involves several challenges and key factors. First, the proactive wrapper needs to be a plug-and-play module that can be applied to both GOD and COD detectors. Secondly, the encryption process should be intuitive to benefit the object detection task. *e.g.*, an ideal template for detection should highlight the foreground objects in the input image. Lastly, the choice of supervision to estimate the template for encryption is hard to formulate.

Previous proactive methods [1, 2] use learnable but image-independent templates for manipulation and localization tasks. However, the object detection task is scene-specific; therefore, the ideal template should be image-dependent. Based on this key insight, we propose a novel plug-and-play proactive wrapper in which we apply object detectors to enhance detection performance. The PrObE D wrapper utilizes an encoder network to learn an image-dependent template. The learned template encrypts the input images by applying a transformation, defined as an element-wise multiplication between the template and the input image. The decoder network recovers the templates from the encrypted images. We utilize regression losses for supervision and leverage the ground-truth object map to guide the learning process, thereby imparting valuable object semantics to be integrated into the template. We then fine-tune the proactive wrapper with the GOD and COD detectors to improve their detection performance. Extensive experiments on MS-COCO, CAMO, COD10K, and NC4K datasets show that PrObE D improves the detection performance for both GOD and COD detectors.

In summary, the contributions of this work include:

- We propose a novel proactive approach *PrObE D* for the object detection task. To the best of our knowledge, this is the first work to develop a proactive approach to 2D object detection.
- We mathematically prove that the proactive method results in a better-converged model than the passive detector under assumptions and, consequently, a better object detector.
- PrObE D wraps around both GOD and COD detectors and improves detection performance on MS-COCO, CAMO, COD10K, and NC4K datasets

## 2 Related works

**Proactive Schemes.** Earlier works adopt to add signals like perturbation [60], adversarial noise [59], and one-hot encoding [68] messages while focusing on tasks like disruption [59, 60] and deepfake tagging [68]. Asnani *et al.* [1] propose to learn an optimized template for binary detection by unseen generative models. Recently, MaLP [2] adds the learnable template to perform generalized

**Table 1:** Comparison of PrObeD with prior works.

Method	Proactive	Task	Template		COD	GOD	Plug-Play
			Number	Type			
Faster R-CNN [58]	×	Object Detection	-	-	×	✓	×
YOLO [52]	×	Object Detection	-	-	×	✓	×
DeTR [8]	×	Object Detection	-	-	×	✓	×
DGNet [34]	×	Object Detection	-	-	✓	×	×
SINet-v2 [17]	×	Object Detection	-	-	✓	×	×
JCSOD [40]	×	Object Detection	-	-	✓	×	×
OGAN [60]	✓	Disrupt	1	Learnable	-	-	×
Ruiz <i>et al.</i> [59]	✓	Disrupt	1	Learnable	-	-	×
Yeh <i>et al.</i> [71]	✓	Disrupt	1	Learnable	-	-	×
FakeTagger [68]	✓	Tagging	$\geq 1$	Fixed, Id-dependent	-	-	×
Asnani <i>et al.</i> [1]	✓	Manipulation Detection	$\geq 1$	Learnable set, Image-independent	-	-	✓
MaLP [2]	✓	Manipulation Localization	$\geq 1$	Learnable set, Image-independent	-	-	✓
PrObeD (Ours)	✓	Object Detection	$\geq 1$	Learnable, Image-dependent	✓	✓	✓

manipulation localization for unknown generative models. Unlike these works, PrObeD uses image-dependent templates and is a plug-and-play wrapper for a different task of object detection.

**Generic Object Detection** Detection of generic objects, instead of specific object categories such as pedestrians [7], apples [13], and others [4, 37, 38], has been a long-standing objective of computer vision. RCNN [24, 25] employs the extraction of object proposals. He *et al.* [31] propose a spatial pooling layer to extract a fixed-length representation of all the objects. Modifications of RCNN [23, 41, 58, 72] increase the inference speed. Feature pyramid network [42] detects objects with a wide variety of scales. The above methods are mostly two-stage, so inference is an issue. Single-stage detectors like YOLO [5, 52–54, 66], SSD [46], HRNet [67] and RetinaNet [43] increase the speed and simplicity of the framework compared to the two-stage detector. Recently, transformer-based methods [8, 74] use a global-scale receptive field. Chen *et al.* [10] use diffusion models to denoise noisy boxes at every forward step. PrObeD functions as a wrapper around the pre-existing object detector, facilitating its transformation into an enhanced object detector. The comparison of PrObeD with prior works is summarized in Tab. 1.

**Camouflaged Object Detection** Early COD works rely on hand-crafted features like co-occurrence matrices [61], 3D convexity [50], optical flow [33], covariance matrix [35], and multivariate calibration components [57]. Later on, [9, 63] incorporate an attention-based cross-level fusion of multi-scale features to recover contextual information. Mei *et al.* [49] take motivation by predators to identify camouflaged objects using a position and focus ideology. SINet [18] uses a search and identification module to perform localization. SINET-v2 [17] uses group-reversal attention to extract the camouflaged maps. [36] explores uncertainty maps and [75] utilizes cube-like architecture to integrate multi-layer features. ANet [39], LSR [47], and JCSOD [40] employ joint learning with different tasks to improve COD. Lately, [12, 48, 70] apply a transformer-based architecture for difficult-aware learning, uncertainty modeling, and temporal consistency. Zhai *et al.* [73] use a graph learning model to disentangle input into different features for localization. DGNet [34] uses image gradients to exploit intensity changes in the camouflaged object from the background. Unlike these methods, PrObeD uses proactive methods to improve camouflaged object detection.

### 3 Proposed Approach

Our method originates from understanding what makes proactive schemes effective. We first overview the two detection problems: GOD and COD in Sec. 3.1. We next derive Lemma 1, where we show that the proactive schemes with the multiplicative transformation of images are better than passive schemes by comparing the deviation of trained network weights from the optimal. Based on this result, we derive that Average Precision (AP) from the proactive model is better than AP from the passive model in Theorem 1. At last, we present our proactive scheme-based wrapper, PrObeD, in Sec. 3.3, which builds upon the Theorem 1 to improve generic 2D objects and camouflaged detection.

### 3.1 Background

#### 3.1.1 Passive Object Detection

Although generic 2D object detection and camouflage detection are similar problems, they have different objective functions. Therefore, we treat them as two different problems and define their objectives separately.

**Generic 2D Object Detection.** Let  $\mathbf{I}_j$  be the set of input images given to the generic 2D object detector  $\mathcal{O}$  with trainable parameters  $\theta$ . Most of these detectors output two sets of predictions per image: (1) bounding box coordinates,  $\mathcal{O}(\mathbf{I}_j)_1 = \hat{T} \in \mathbb{R}^4$ , (2) class logits,  $\mathcal{O}(\mathbf{I}_j)_2 = \hat{C} \in \mathbb{R}^C$ , where  $N$  is the number of foreground object categories. If the ground-truth bounding box coordinates are  $T_j$ , and the ground-truth category label is  $C$ , the objective function of such detector is:

$$\min_{\theta} \left\{ \sum_j \left( \|\mathcal{O}(\mathbf{I}_j; \theta)_1 - T_j\|_2 \right) - \sum_j \sum_{i=1}^N \left( C_j^i \cdot \log(\mathcal{O}(\mathbf{I}_j; \theta)_2) \right) \right\}. \quad (1)$$

**Camouflaged Object Detection.** Let  $\mathbf{I}_j$  be the input image set given to the camouflaged object detector  $\mathcal{O}$  with trainable parameters  $\theta$ , and  $\mathbf{G}_j$  be the ground-truth segmentation map. Prior passive works predict a segmentation map with the following objective:

$$\min_{\theta} \left\{ \sum_j \left( \|\mathcal{O}(\mathbf{I}_j; \theta) - \mathbf{G}_j\|_2 \right) \right\}. \quad (2)$$

#### 3.1.2 Proactive Object Detection

Proactive schemes [1, 2] encrypt the input images with the template to aid manipulation detection/localization. Such schemes take an input image  $\mathbf{I}_j \in \mathbb{R}^{H \times W \times 3}$  and learn a template  $\mathbf{S}_j \in \mathbb{R}^{H \times W}$ . PrObeD uses image-dependent templates to improve object detection. Given an input image  $\mathbf{I}_j \in \mathbb{R}^{H \times W \times 3}$ , PrObeD learns to output a template  $\mathbf{S}_j \in \mathbb{R}^{H \times W}$ , which can be used by a transformation  $\mathcal{T}$  resulting in encrypted images  $\mathcal{T}(\mathbf{I}_j)$ . PrObeD uses element-wise multiplication as the transformation  $\mathcal{T}$ , which is defined as:

$$\mathcal{T}(\mathbf{I}_j) = \mathcal{T}(\mathbf{I}_j; \mathbf{S}_j) = \mathbf{I}_j \odot \mathbf{S}_j. \quad (3)$$

### 3.2 Mathematical Analysis of Passive and Proactive Detectors

PrObeD optimizes the template to improve the performance of the object detector. We argue that this template helps arrive at a better global minima representing the optimal parameters  $\theta$ . We now define the following lemma to support our argument:

**Lemma 1. Converged weights of proactive and passive detectors.** Consider a linear regression model that regresses an input image  $\mathbf{I}_j$  under an additive noise setup to obtain the 2D coordinates. Assume the noise under consideration  $e$  is a normal random variable  $\mathcal{N}(0, \sigma^2)$ . Let  $\mathbf{w}$  and  $\mathbf{w}^*$  denote the trained weights of the pretrained linear regression model and the optimal weights of the linear regression model. Also, assume SGD optimizes the model parameters with decreasing step size  $s$  such that the steps are square summable i.e.,  $S = \lim_{t \rightarrow \infty} \sum_{k=1}^t s_k^2$  exist, and the noise is independent of the image. Then, there exists a template  $\mathbf{S}_j \in [0, 1]$  for the image  $\mathbf{I}_j$  such that the multiplicative transformation of images as the input results in a trained weight  $\mathbf{w}'$  closer to the optimal weight than the originally trained weight  $\mathbf{w}$ . In other words,

$$\mathbb{E}(\|\mathbf{w}' - \mathbf{w}^*\|_2) < \mathbb{E}(\|\mathbf{w} - \mathbf{w}^*\|_2). \quad (4)$$

The proof of Lemma 1 is in supplementary. We use the variance of the gradient of the encrypted images to arrive at this lemma. We next use Lemma 1 to derive the following theorem:

**Theorem 1. AP comparison of proactive and passive detectors.** Consider a linear regression model that regresses an input image  $\mathbf{I}_j$  under an additive noise setup to obtain the 2D coordinates. Assume the noise under consideration  $e$  is a normal random variable  $\mathcal{N}(0, \sigma^2)$ . Let  $\mathbf{w}$  and  $\mathbf{w}^*$  denote the

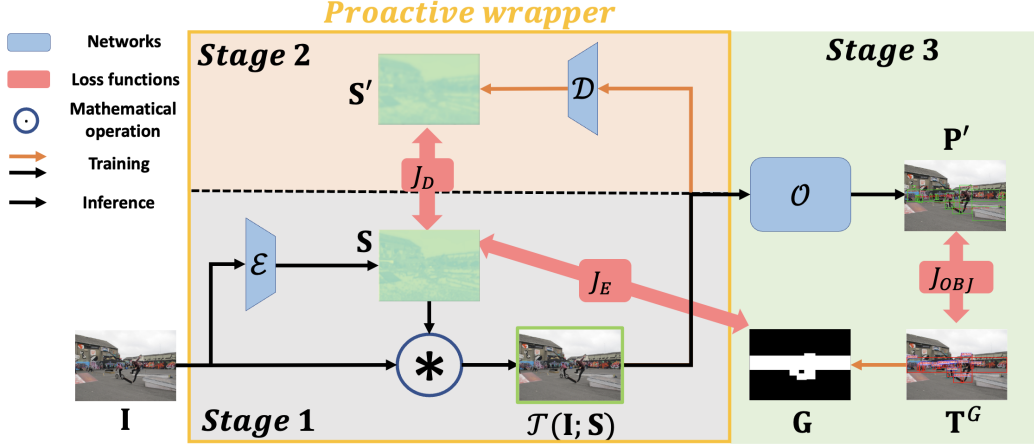


**Figure 2: Overview of PrObE.** PrObE consists of three stages: (1) template generation, (2) template recovery, and (3) detector fine-tuning. The templates are generated by encoder network  $\mathcal{E}$  to encrypt the input images. The decoder network  $\mathcal{D}$  is used to recover the template from the encrypted images. Finally, the encrypted images are used to fine-tune the object detector to perform detection. We train all the stages in an end-to-end manner. However, for inference, we only use stages 1 and 3. Best viewed in color.

trained weights of the pretrained linear regression model and the optimal weights of the linear regression model. Also, assume SGD optimizes the model parameters with decreasing step size  $s$  such that the steps are square summable i.e.,  $\mathcal{S} = \lim_{t \rightarrow \infty} \sum_{k=1}^t s_k^2$  exist, and the noise is independent of the image. Then, the AP of the proactive detector is better than the AP of the passive detector.

The proof of Theorem 1 is in the supplementary. We use the Lemma 1 and the non-decreasing nature of AP w.r.t. IoU to arrive at this theorem. Next, we adapt the objectives of Eqs. (1) and (2) to incorporate the proactive methods as follows:

$$\min_{\theta, \mathcal{S}_j} \left\{ \sum_j \left( \left\| \mathcal{O}(\mathcal{T}(\mathbf{I}_j; \mathcal{S}_j); \theta)_1 - T_j \right\|_2 \right) - \sum_j \sum_{i=1}^N \left( C_j^i \cdot \log(\mathcal{O}(\mathcal{T}(\mathbf{I}_j; \mathcal{S}_j); \theta)_2) \right) \right\}, \quad (5)$$

$$\min_{\theta, \mathcal{S}_j} \left\{ \sum_j \left( \left\| \mathcal{O}(\mathcal{T}(\mathbf{I}_j; \mathcal{S}_j); \theta) - \mathbf{G}_j \right\|_2 \right) \right\}. \quad (6)$$

### 3.3 PrObE

Our proposed approach comprises of three stages: template generation, template recovery, and detector fine-tuning. First, we use an encoder network to generate an image-dependent template for image encryption. This encrypted image is further used to recover the template through a decoder network. Finally, the object detector is fine-tuned using the encrypted images. All three stages are trained in an end-to-end fashion. While all the stages are used for training PrObE, we specifically use only stages 1 and 3 for inference. We will now describe each stage in detail.

#### 3.3.1 Proactive Wrapper

Our proposed approach consists of three stages, as shown in Fig. 2. However, only the first two stages are part of our proposed proactive wrapper, which can be applied to object detector to improve its performance.

**Stage 1: Template Generation.** Prior works learn a set of templates [1,2] in their proactive schemes. This set of templates is enough to perform the respective downstream tasks as the generative model manipulates the template, which is easy to capture with a set of learnable templates. However, for object detection tasks, every image has unique object characteristics such as size, appearance, and color that can vary significantly. This variability present in the images may exceed the descriptive capacity of a finite set of templates, thereby necessitating the use of image-specific templates to

accurately represent the range of object features present in each image. In other words, a fixed set of templates may not be sufficiently flexible to capture the diversity of visual features across the given set of input images, thus demanding more adaptable, image-dependent templates.

Motivated by the above argument, we propose to generate the template  $\mathbf{S}_j$  for every image using an encoder network. We hypothesize that highlighting the area of the key foreground objects would be beneficial for object detection. Therefore, for GOD, we use the ground-truth bounding boxes  $T^G$  to generate the pseudo ground-truth segmentation map. Specifically, for any image  $\mathbf{I}_j$ , if the bounding box coordinates are  $T_j^G = \{x_1, x_2, y_1, y_2\}$ , we define the pseudo ground-truth segmentation map as:

$$\forall m \in [0, H], n \in [0, W], \text{ we have} \\ \mathbf{G}_j(m, n) = 1 \text{ if } x_1 \leq m \leq x_2 \text{ and } y_1 \leq n \leq y_2, \text{ otherwise } 0$$

However, for COD, the dataset already has the ground-truth segmentation map  $\mathbf{G}_j$ , which we use as the supervision for the encoder to output the templates with semantic information of the image to be restricted only in the region of interest for the detector. For both GOD and COD, we minimize the cosine similarity (Cos) between  $\mathbf{S}_j$  and  $\mathbf{G}_j$  as the supervision for the encoder network. The encoder loss  $J_E$  is as follows:

$$J_E = 1 - \text{Cos}(\mathbf{S}_j, \mathbf{G}_j) = 1 - \text{Cos}(\mathcal{E}(\mathbf{I}_j), \mathbf{G}_j). \quad (7)$$

This generated template acts as a mask for the input image to highlight the object region of interest for the detector. We use this template with the transformation  $\mathcal{T}$  to encrypt the input image as  $\mathcal{T}(\mathbf{I}_j; \mathbf{S}_j) = \mathbf{I}_j \odot \mathbf{S}_j$ . As we start from the pretrained model of object detector  $\mathcal{O}$ , we initialize the bias of the last layer of the encoder as 0 so that for the first few iterations,  $\mathbf{S}_j \approx \mathbf{1}$ . This is to ensure that the distribution of  $\mathbf{I}_j$  and  $\mathcal{T}(\mathbf{I}_j; \mathbf{S}_j)$  remains similar for the first few iterations, and  $\mathcal{O}$  doesn't encounter a sudden change in its input distribution.

**Stage 2: Template Recovery.** So far, we have discussed the generation of template  $\mathbf{S}_j$  using  $\mathcal{E}$ , which will be used as a mask to encrypt the input image. The encrypted images are used for two purposes: (1) recovery of templates and (2) fine-tuning of the object detector. The main intuition of recovering the templates is from the prior works on image steganalysis [55, 56] and proactive schemes [1, 2]. Motivated by these works, we draw the following insight: *“To properly learn the optimal template and embed it onto the input images, it is beneficial to recover the template from encrypted images.”*

To perform recovery, we exploit an encoder-decoder approach. Using this approach leverages the strengths of the encoder network  $\mathcal{E}$  for feature extraction, capturing the most useful salient details, and the decoder network  $\mathcal{D}$  for information recovery, allowing for efficient and effective encryption and decryption of the template. We also empirically show that not using the decoder to recover the templates harms the object detection performance.

To supervise  $\mathcal{D}$  in recovering  $\mathbf{S}_j$  from  $\mathcal{T}(\mathbf{I}_j; \mathbf{S}_j)$ , we propose to maximize the cosine similarity between the recovered template,  $\mathbf{S}'_j$  and  $\mathbf{S}_j$ . The decoder loss is as follows:

$$J_D = 1 - \text{Cos}(\mathbf{S}'_j, \mathbf{S}_j) = 1 - \text{Cos}(\mathcal{D}(\mathcal{T}(\mathbf{I}_j; \mathbf{S}_j)), \mathbf{S}_j). \quad (8)$$

**Stage 3: Detector Fine-tuning.** Due to our encryption, the distribution of the images input to the pretrained  $\mathcal{O}$  changes. Thus, we fine-tune  $\mathcal{O}$  on the encrypted images  $\mathcal{T}(\mathbf{I}_j; \mathbf{S})$ . As proposed in Theorem 1, given the encrypted images  $\mathcal{T}(\mathbf{I}_j; \mathbf{S})$ , we use the pretrained detector  $\mathcal{O}$  with parameters  $\theta$  to arrive at a better local minima. Therefore, the general objective of GOD and COD in Eq. (5) and Eq. (6) change to as follows:

$$\min_{\theta, \theta_{\mathcal{E}}, \theta_{\mathcal{D}}} \left\{ \sum_j \left( \|\mathcal{O}(\mathcal{T}(\mathbf{I}_j; \mathcal{E}(\mathbf{I}_j; \theta_{\mathcal{E}})); \theta, \theta_{\mathcal{D}})_1 - T_j\|_2 - \sum_{i=1}^N (C_j^i \cdot \log(\mathcal{O}(\mathcal{T}(\mathbf{I}_j; \mathcal{E}(\mathbf{I}_j; \theta_{\mathcal{E}})); \theta, \theta_{\mathcal{D}})_2)) \right) \right\}, \quad (9)$$

$$\min_{\theta, \theta_{\mathcal{E}}, \theta_{\mathcal{D}}} \left\{ \sum_j \left( \left\| \mathcal{O}(\mathcal{T}(\mathbf{I}_j; \mathcal{E}(\mathbf{I}_j; \theta_{\mathcal{E}})); \theta, \theta_{\mathcal{D}}) - \mathbf{G}_j \right\|_2 \right) \right\}. \quad (10)$$

We use the detector-specific loss function  $J_{OBJ}$  of  $\mathcal{O}$  along with the encoder and decoder loss in Eq. (7) and Eq. (8) to train all the three stages. The overall loss function  $J$  to train PrObE is as follows:

$$J = \lambda_{OBJ} J_{OBJ} + \lambda_E J_E + \lambda_D J_D. \quad (11)$$



**Table 2: GOD results** on MS-COCO val split. PrObeD improves the performance of all GOD at all thresholds and across all categories.

Method	AP $\uparrow$	AP <sub>50</sub> $\uparrow$	AP <sub>75</sub> $\uparrow$	AP <sub>S</sub> $\uparrow$	AP <sub>M</sub> $\uparrow$	AP <sub>L</sub> $\uparrow$
Faster R-CNN [58]	19.3	42.5	16.9	1.8	17.9	39.3
Faster R-CNN [58]+PrObeD	<b>31.7</b>	<b>52.6</b>	<b>33.3</b>	<b>11.0</b>	<b>35.5</b>	<b>51.1</b>
Faster R-CNN + FPN [42]	37.3	58.0	40.6	21.4	41.0	48.4
Faster R-CNN + FPN [42] + Seg. Mask [30]	38.2	60.3	41.7	22.1	43.2	<b>51.2</b>
Faster R-CNN + FPN [42] + PrObeD	<b>38.5</b>	<b>60.4</b>	<b>41.9</b>	<b>22.5</b>	<b>43.4</b>	49.8
Sparse R-CNN [62]	37.6	55.6	40.2	20.5	39.6	52.9
Sparse R-CNN [62]+ PrObeD	<b>39.2</b>	<b>57.5</b>	<b>41.5</b>	<b>21.7</b>	<b>40.1</b>	<b>53.6</b>
YOLOv5 [52]	48.9	67.6	53.1	31.8	54.4	62.3
YOLOv5 [52]+ PrObeD	<b>49.4</b>	<b>67.9</b>	<b>53.5</b>	<b>32.0</b>	<b>55.1</b>	<b>62.6</b>
DeTR [8]	41.9	62.3	44.1	20.3	45.8	61.0
DeTR [8]+ PrObeD	<b>42.1</b>	<b>62.6</b>	<b>44.4</b>	<b>20.4</b>	<b>46.0</b>	<b>61.3</b>

**Table 3: COD results** on CAMO, COD10K and NC4K datasets. PrObeD outperforms DGNet on all datasets and metrics.

Method	CAMO				COD10K				NC4K			
	$E_m \uparrow$	$S_m \uparrow$	$wF_\beta \uparrow$	$MAE \downarrow$	$E_m \uparrow$	$S_m \uparrow$	$wF_\beta \uparrow$	$MAE \downarrow$	$E_m \uparrow$	$S_m \uparrow$	$wF_\beta \uparrow$	$MAE \downarrow$
DGNet [34]	0.859	0.791	0.681	0.079	0.833	0.776	0.603	0.046	0.876	0.815	0.710	0.059
+ PrObeD	<b>0.871</b>	<b>0.797</b>	<b>0.702</b>	<b>0.071</b>	<b>0.869</b>	<b>0.803</b>	<b>0.661</b>	<b>0.037</b>	<b>0.900</b>	<b>0.838</b>	<b>0.755</b>	<b>0.049</b>

## 4 Experiments

We apply PrObeD for two categories of object detectors: GOD and COD.

**GOD Baselines.** For GOD, we apply PrObeD on four detectors with varied architectures: two-stage, one-stage, and transformer-based detectors, namely, Faster R-CNN [58], YOLO [52], Sparse R-CNN, and DeTR [8]. We use these works as baselines for three reasons: (1) varied architecture types, (2) their increased prevalence in the community, and (3) varied timelines (from earlier to recent detectors). We use the PyTorch [51] code of the respective detectors for our GOD experiments and use the corresponding GODs as our baseline. For YOLOv5 and DeTR, we use the official repositories released by the authors; for Faster R-CNN, we use the public repository "Faster R-CNN.pytorch". For other GOD detectors, we use Detectron2 library as the pre-trained detector. We use the ResNet101 backbone for Faster R-CNN, Sparse R-CNN and DeTR, and CSPDarknet53 for YOLOv5.

**COD Baselines.** For COD, we apply PrObeD on the current SoTA camouflage detector DGNet [34] and use DGNet as our baseline. For all object detectors, we use the pretrained model released by the authors and fine-tune them with PrObeD. Please see the supplementary for more details.

**Datasets.** Our experiments use the MS-COCO 2017 [44] dataset for GOD, while we use CAMO [39], COD10K [17], and NC4K [47] datasets for COD. We use the following splits of these datasets:

- MS-COCO 2017 Val Split [44]: It includes 118,287 images for training and 5K for testing.
- COD10K Val Split [17]: It includes 4,046 camouflaged images for training and 2,026 for testing.
- CAMO Val Split [39]: It includes 1K camouflaged images for training and 250 for testing.
- NC4K Val [47]: It includes 4,121 NC4K images. We use it for generalization testing as in [34].

**Evaluation Metrics.** We use mean average precision average at multiple thresholds in [0.5, 0.95] (AP) for GOD as in [44]. We also report results at threshold of 0.5 (AP<sub>50</sub>), threshold of 0.75 (AP<sub>75</sub>) and at different object sizes: small (AP<sub>S</sub>), medium (AP<sub>M</sub>), and large (AP<sub>L</sub>). For COD, we use E-measure  $E_m$ , S-measure  $S_m$ , weighted F1 score  $wF_\beta$  and mean absolute error  $MAE$  as [34].

### 4.1 GOD Results

**Quantitative Results.** Tab. 2 shows the results of applying PrObeD on GOD networks. PrObeD improves the average precision of all three detectors. The performance gain is significant for Faster R-CNN. As Faster R-CNN is an older detector, it was at a worse minima to start with. PrObeD improves the convergence weight of Faster R-CNN by a significant margin, thereby improving the performance. We further experiment with two variations of Faster R-CNN, namely, Faster R-CNN +

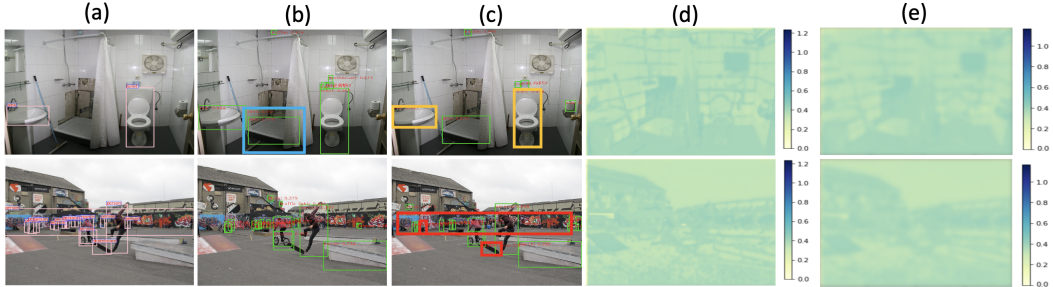


**Figure 3: Qualitative GOD Results** on MS-COCO 2017 dataset. (a) ground-truth annotations, (b) Faster R-CNN [58] predictions, (c) Faster R-CNN [58]+ PrObE predictions, (d) generated template, and (e) recovered template. We highlight the objects responsible for improvement in (c) as compared to (b). The yellow box represents better localization, the blue box represents false positives, and the red box represents missed predictions. PrObE improves on all these errors made by (b).

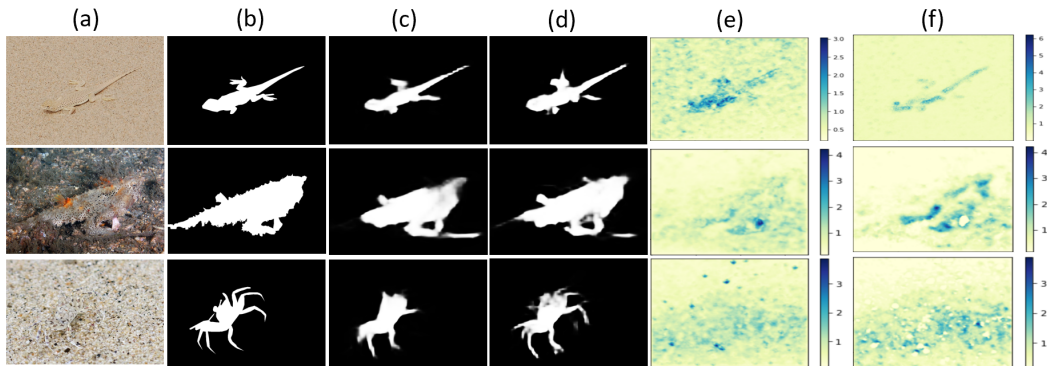


**Figure 4: Qualitative COD Results** on CAMO, COD10K, and NC4K datasets from top to bottom, after applying PrObE. (a) input images, (b) ground-truth camouflaged map, (c) DGNNet [34] predictions, (d) DGNNet [34]+ PrObE predictions, (e) generated PrObE template, and (f) recovered PrObE template. PrObE template has the semantics of the camouflaged object, which aids DGNNet in detection.

FPN and Sparse-RCNN. We observe an increase in the performance of both detectors. PrObE also improves newer detectors like YOLOv5 and DeTR, although the gains are smaller compared to Faster R-CNN. We believe this happens because the newer detectors leave little room for improvement due to which PrObE improves the performance slightly. We next compare PrObE with a work that leverage segmentation map as a mask for object detection. We compare our performance with Mask R-CNN [30], which uses an image segmentation branch to help with object detection. Tab. 2 shows that the gains using Mask R-CNN are lower than using our proactive wrapper.

**Qualitative Results.** Fig. 3 shows qualitative results for the MS-COCO 2017 dataset. PrObE clearly improves the performance of pretrained Faster R-CNN for three types of errors: Missed predictions, false negatives, and localization errors. PrObE has a lower number of missed predictions, fewer false positives, and better bounding box localization. We also visualize the generated and recovered templates. We see that the template has object semantics of the input images. When the template is multiplied with the input image, it highlights the foreground objects, thereby making the task of object detector easier.

**Error Analysis.** We show the error analysis [6] for GOD section 4 of the supplementary. We observe that all GOD detectors make mistakes mainly due to five types of errors: classification, localization, duplicate detection, background detection, and missed detection. The main reason for the degraded performance is the errors in which the foreground-background boundary is missed. These errors include localization, background detection, and missed detection. Our proactive wrapper significantly corrects these errors, as the template has object semantics, which, when multiplied with the input image, highlights the foreground objects, consequently simplifying the task of object detection.



**Table 4:** Performance comparison with proactive works. MaLP [2] has a significantly deteriorated performance than PrObeD.

Method	CAMO				COD10K				NC4K			
	$E_m \uparrow$	$S_m \uparrow$	$wF_\beta \uparrow$	MAE $\downarrow$	$E_m \uparrow$	$S_m \uparrow$	$wF_\beta \uparrow$	MAE $\downarrow$	$E_m \uparrow$	$S_m \uparrow$	$wF_\beta \uparrow$	MAE $\downarrow$
MaLP [2]	0.474	0.514	0.218	0.254	0.491	0.520	0.150	0.202	0.503	0.548	0.228	0.222
PrObeD	<b>0.871</b>	<b>0.797</b>	<b>0.702</b>	<b>0.071</b>	<b>0.869</b>	<b>0.803</b>	<b>0.661</b>	<b>0.037</b>	<b>0.900</b>	<b>0.838</b>	<b>0.755</b>	<b>0.049</b>

**Table 5: Ablation studies** of PrObeD using Faster R-CNN GOD on MS-COCO 2017 dataset. Removing the encoder/decoder network or adding the template results in degraded performance.

Changed	From $\rightarrow$ To	AP $\uparrow$	AP <sub>50</sub> $\uparrow$	AP <sub>75</sub> $\uparrow$	AP <sub>S</sub> $\uparrow$	AP <sub>M</sub> $\uparrow$	AP <sub>L</sub> $\uparrow$
Template	Image Dependent $\rightarrow$ Fixed	17.6	37.9	15.1	1.3	15.4	39.5
	Image Dependent $\rightarrow$ Universal	19.4	42.6	17.1	1.9	18.0	39.4
Decoder	Yes $\rightarrow$ No	25.2	46.1	26.2	5.3	26.6	24.1
Transformation	Multiply $\rightarrow$ Add	19.2	42.3	20.1	1.7	17.9	39.1
PrObeD	-	<b>31.7</b>	<b>52.6</b>	<b>33.3</b>	<b>11.0</b>	<b>35.5</b>	<b>51.1</b>

## 4.2 COD Results

**Quantitative Results.** Tab. 3 shows the result of applying PrObeD to DGNNet [34] on three different datasets. PrObeD, when applied on top of DGNNet, outperforms DGNNet on all four metrics for all datasets. The biggest gain appears in COD10K and NC4K datasets. This is impressive as these datasets have more diverse testing images than CAMO. As NC4K is only a testing set, the higher performance of PrObeD demonstrates its superior generalizability as compared to DGNNet [34]. This result agrees with the observation in [1, 2], where proactive-based approaches exhibit improved generalization on manipulation detection and localization tasks.

**Qualitative Results.** Fig. 4 visualizes the predicted camouflaged map for DGNNet before and after applying PrObeD on testing samples of all three datasets. PrObeD improves the predicted camouflaged map, with less blurriness along the boundaries and better localization of the camouflaged object. As observed before for GOD, the generated and recovered template has the semantics of the camouflaged objects, which after multiplication intensifies the foreground object, resulting in better segmentation by DGNNet.

## 4.3 Ablation Study

**Comparison with Proactive Works.** The prior proactive works perform a different task of image manipulation detection and localization. Therefore, these works are not directly comparable to our proposed proactive wrapper, which performs a different task of object detection as described in Tab. 1. However, manipulation localization and COD both involve a prediction of a localization map, segmentation, and fakeness map, respectively. This inspires us to experiment with MaLP [2] for the task of COD. We train the localization module of MaLP supervised with the COD datasets. The results are shown in Tab. 4. We see that MaLP is not able to perform well for all three datasets. MaLP is designed for estimating universal templates rather than templates tailored to specific images. It shows the significance of image-specific templates in object detection. While MaLP’s design with image-independent templates is effective for localizing image manipulation, applying it to object detection has a negative impact on performance.

**Framework Design.** PrObeD consists of blocks to improve the object detector. Tab. 5 ablates different versions of PrObeD to highlight the importance of each block in our design. PrObeD utilizes an encoder network  $\mathcal{E}$  to learn image-dependent templates aiding the detector. We remove the encoder  $\mathcal{E}$  from our network, replacing it with a fixed template. We observe that the performance deteriorates by a large margin. Next, we make this template learnable as proposed in PrObeD, but only a single template would be used for all the input images. This choice also results in worse performance, highlighting that image-dependent templates are necessary for object detection. Finally, we remove the decoder network  $\mathcal{D}$ , which is used to recover the template from the encrypted images. Although this results in a better performance than the pretrained Faster R-CNN, we observe a drop as compared to PrObeD. Therefore, as discussed in Sec. 3.3, the recovery of templates is indeed a necessary and beneficial step for boosting the performance of the proactive schemes.

**Table 6: Ablation of training iterations** on Faster R-CNN, YOLOv5, and DeTR for more iterations similar to after applying PrObED. We also report the inference time for all the detectors before and after applying PrObED. Training object detectors proactively with PrObED results in more performance gain compared to training passively for more iterations. PrObED adds an overhead cost on top of the inference cost of detectors.

Method	Iterations	AP $\uparrow$	AP <sub>50</sub> $\uparrow$	AP <sub>75</sub> $\uparrow$	AP <sub>S</sub> $\uparrow$	AP <sub>M</sub> $\uparrow$	AP <sub>L</sub> $\uparrow$	Time (ms)
Faster R-CNN [58]	1 $\times$	19.3	42.5	16.9	1.8	17.9	39.3	161.1
Faster R-CNN [58]	2 $\times$	20.1	46.6	21.5	3.3	20.3	41.2	
Faster R-CNN [58] + PrObED	2 $\times$	<b>31.7</b>	<b>52.6</b>	<b>33.3</b>	<b>11.0</b>	<b>35.5</b>	<b>51.1</b>	175.3 ( $\uparrow$ 8.7%)
YOLOv5 [52]	1 $\times$	48.9	67.6	53.1	31.8	54.4	62.3	48.5
YOLOv5 [52]	2 $\times$	48.8	67.7	53.0	31.8	54.7	62.4	
YOLOv5 [52] + PrObED	2 $\times$	<b>49.4</b>	<b>67.9</b>	<b>53.5</b>	<b>32.0</b>	<b>55.1</b>	<b>62.6</b>	62.7 ( $\uparrow$ 29.1%)
DeTR [8]	1 $\times$	41.9	62.3	44.1	20.3	45.8	61.0	194.2
DeTR [8]	2 $\times$	41.9	62.4	44.0	20.1	45.9	61.1	
DeTR [8] + PrObED	2 $\times$	<b>42.1</b>	<b>62.6</b>	<b>44.4</b>	<b>20.4</b>	<b>46.0</b>	<b>61.3</b>	208.4 ( $\uparrow$ 7.2%)

**Encryption Process.** PrObED includes an encryption process as described in Eq. (3), which involves multiplying the template with the input image. This process makes the template act as a mask, highlighting the foreground for better detection. However, prior proactive works [1, 2] consider adding templates to achieve better results. Thus, we ablate by changing the encryption process to template addition. Tab. 5 shows that template addition degrades performance by a significant margin w.r.t. our multiplication scheme. This shows that encryption is a key step in formulating proactive schemes, and the same encryption process may not work for all tasks.

**More Training Time.** We perform an ablation to show that the performance gain of the detector is due to our proactive wrapper instead of training for more iterations of the pretrained object detector. Results in Tab. 6 show that although more training iterations for the detector has a performance gain, it’s not enough to get the significant margin in performance as achieved by PrObED. This shows that extra training can help, but only up to a certain extent.

**Inference Time.** We evaluate the overhead computational cost after applying PrObED on different object detectors are shown in Tab. 6, averaged across 1,000 images, on a NVIDIA V100 GPU. Our encoder network has 17 layers, which adds extra cost for inference. For detectors with bulky architectures like Faster R-CNN (ResNet101) and DeTR (transformer), the overhead computational cost is quite small, 8.7% and 7.2%, respectively. This additional cost is minor compared to the performance gain of detectors, especially Faster R-CNN. For a lighter detector like YOLOv5, our overhead computational cost increases to 29.1%. So, there is a trade-off of applying PrObED to different detectors with varied architectures. PrObED is more beneficial to bulky detectors like two-staged/transformer-based as compared to one-stage detectors.

## 5 Conclusion

We mathematically prove that the proactive method results in a better-converged model than the passive detector under assumptions and, consequently, a better 2D object detector. Based on this finding, we propose a proactive scheme wrapper, PrObED, which enhances the performance of camouflaged and generic object detectors. The wrapper outputs an image-dependent template using an encoder network, which encrypts the input images. These encrypted images are then used to fine-tune the object detector. Extensive experiments on MS-COCO, CAMO, COD10K, and NC4K datasets show that PrObED improves the overall object detection performance for both GOD and COD detectors.

**Limitations.** Our proposed scheme has the following limitations. First, PrObED does not provide a significant gain for recent object detectors such as YOLO and DeTR. Second, the proactive wrapper should be thoroughly tested on other object detectors to show the generalizability of PrObED. Finally, we only experiment with simple multiplication and addition as the encryption scheme. A more sophisticated encryption process might further improve the object detectors’ performance. We leave these for our future avenues.

## References

- [1] Vishal Asnani, Xi Yin, Tal Hassner, Sijia Liu, and Xiaoming Liu. Proactive image manipulation detection. In *CVPR*, 2022. 1, 2, 3, 4, 5, 6, 9, 10, 17
- [2] Vishal Asnani, Xi Yin, Tal Hassner, and Xiaoming Liu. MaLP: Manipulation localization using a proactive scheme. In *CVPR*, 2023. 1, 2, 3, 4, 5, 6, 9, 10, 17
- [3] Vishal Asnani, Xi Yin, Tal Hassner, and Xiaoming Liu. Reverse engineering of generative models: Inferring model hyperparameters from generated images. *TPAMI*, 2023.
- [4] Yousef Atoum, Joseph Roth, Michael Bliss, Wende Zhang, and Xiaoming Liu. Monocular video-based trailer coupler detection using multiplexer convolutional neural network. In *ICCV*, 2017. 3
- [5] Alexey Bochkovskiy, Chien-Yao Wang, and Hong-Yuan Mark Liao. YOLOv4: Optimal speed and accuracy of object detection. *arXiv preprint arXiv:2004.10934*, 2020. 1, 3
- [6] Daniel Bolya, Sean Foley, James Hays, and Judy Hoffman. TIDE: A general toolbox for identifying object detection errors. In *ECCV*, 2020. 8, 17
- [7] Garrick Brazil and Xiaoming Liu. Pedestrian detection with autoregressive network phases. In *CVPR*, 2019. 3
- [8] Nicolas Carion, Francisco Massa, Gabriel Synnaeve, Nicolas Usunier, Alexander Kirillov, and Sergey Zagoruyko. End-to-end object detection with transformers. In *ECCV*, 2020. 1, 3, 7, 10
- [9] Geng Chen, Si-Jie Liu, Yu-Jia Sun, Ge-Peng Ji, Ya-Feng Wu, and Tao Zhou. Camouflaged object detection via context-aware cross-level fusion. *IEEE Transactions on Circuits and Systems for Video Technology*, 32(10), 2022. 1, 3
- [10] Shoufa Chen, Peize Sun, Yibing Song, and Ping Luo. DiffusionDet: Diffusion model for object detection. In *CVPR*, 2023. 1, 3
- [11] Wei-Chen Chen, Xin-Yi Yu, and Lin-Lin Ou. Pedestrian attribute recognition in video surveillance scenarios based on view-attribute attention localization. *Machine Intelligence Research*, 2022. 1
- [12] Xuelian Cheng, Huan Xiong, Deng-Ping Fan, Yiran Zhong, Mehrtash Harandi, Tom Drummond, and Zongyuan Ge. Implicit motion handling for video camouflaged object detection. In *CVPR*, 2022. 3
- [13] Pengyu Chu, Zhaojian Li, Kyle Lammers, Renfu Lu, and Xiaoming Liu. Deepapple: Deep learning-based apple detection using a suppression mask R-CNN. *PRL*, 2021. 3
- [14] Jifeng Dai, Yi Li, Kaiming He, and Jian Sun. R-FCN: Object detection via region-based fully convolutional networks. *NeurIPS*, 2016. 1
- [15] Navneet Dalal and Bill Triggs. Histograms of oriented gradients for human detection. In *CVPR*, 2005. 1
- [16] Mohammad Derakhshani, Saeed Masoudnia, Amir Shaker, Omid Mersa, Mohammad Sadeghi, Mohammad Rastegari, and Babak Araabi. Assisted excitation of activations: A learning technique to improve object detectors. In *CVPR*, 2019. 1
- [17] Deng-Ping Fan, Ge-Peng Ji, Ming-Ming Cheng, and Ling Shao. Concealed object detection. *TPAMI*, 2021. 1, 3, 17
- [18] Deng-Ping Fan, Ge-Peng Ji, Guolei Sun, Ming-Ming Cheng, Jianbing Shen, and Ling Shao. Camouflaged object detection. In *CVPR*, 2020. 1, 3
- [19] Deng-Ping Fan, Ge-Peng Ji, Tao Zhou, Geng Chen, Huazhu Fu, Jianbing Shen, and Ling Shao. Pranut: Parallel reverse attention network for polyp segmentation. In *MICCAI*, 2020. 1
- [20] Pedro Felzenszwalb, David McAllester, and Deva Ramanan. A discriminatively trained, multi-scale, deformable part model. In *CVPR*, 2008. 1
- [21] Sanja Fidler, Roozbeh Mottaghi, Alan Yuille, and Raquel Urtasun. Bottom-up segmentation for top-down detection. In *CVPR*, 2013. 1
- [22] Spyros Gidaris and Nikos Komodakis. Object detection via a multi-region and semantic segmentation-aware cnn model. In *ICCV*, 2015. 1
- [23] Ross Girshick. Fast R-CNN. In *ICCV*, 2015. 1, 3
- [24] Ross Girshick, Jeff Donahue, Trevor Darrell, and Jitendra Malik. Rich feature hierarchies for accurate object detection and semantic segmentation. In *CVPR*, 2014. 1, 3
- [25] Ross Girshick, Jeff Donahue, Trevor Darrell, and Jitendra Malik. Region-based convolutional networks for accurate object detection and segmentation. *TPAMI*, 2015. 3
- [26] Agrim Gupta, Piotr Dollár, and Ross Girshick. LVIS: A dataset for large vocabulary instance segmentation. In *CVPR*, 2019. 1

- [27] Chunming He, Kai Li, Yachao Zhang, Longxiang Tang, Yulun Zhang, Zhenhua Guo, and Xiu Li. Camouflaged object detection with feature decomposition and edge reconstruction. In *CVPR*, 2023. 1
- [28] Chunming He, Kai Li, Yachao Zhang, Guoxia Xu, Longxiang Tang, Yulun Zhang, Zhenhua Guo, and Xiu Li. Weakly-supervised concealed object segmentation with SAM-based pseudo labeling and multi-scale feature grouping. *arXiv preprint arXiv:2305.11003*, 2023. 1
- [29] Chunming He, Kai Li, Yachao Zhang, Yulun Zhang, Zhenhua Guo, Xiu Li, Martin Danelljan, and Fisher Yu. Strategic preys make acute predators: Enhancing camouflaged object detectors by generating camouflaged objects. *arXiv preprint arXiv:2308.03166*, 2023. 1
- [30] Kaiming He, Georgia Gkioxari, Piotr Dollár, and Ross Girshick. Mask R-CNN. In *ICCV*, 2017. 7, 8
- [31] Kaiming He, Xiangyu Zhang, Shaoqing Ren, and Jian Sun. Spatial pyramid pooling in deep convolutional networks for visual recognition. *TPAMI*, 2015. 3
- [32] Yihui He, Chenchen Zhu, Jianren Wang, Marios Savvides, and Xiangyu Zhang. Bounding box regression with uncertainty for accurate object detection. In *CVPR*, 2019. 1, 15
- [33] Jianqin Yin Yanbin Han Wendi Hou and Jinping Li. Detection of the mobile object with camouflage color under dynamic background based on optical flow. *Procedia Engineering*, 2011. 1, 3
- [34] Ge-Peng Ji, Deng-Ping Fan, Yu-Cheng Chou, Dengxin Dai, Alexander Liniger, and Luc Van Gool. Deep gradient learning for efficient camouflaged object detection. *Machine Intelligence Research*, 2023. 1, 3, 7, 8, 9, 17
- [35] Ge-Peng Ji, Lei Zhu, Mingchen Zhuge, and Keren Fu. Fast camouflaged object detection via edge-based reversible re-calibration network. *Pattern Recognition*, 123, 2022. 3
- [36] Nobukatsu Kajiura, Hong Liu, and Shin’ichi Satoh. Improving camouflaged object detection with the uncertainty of pseudo-edge labels. In *ACM Multimedia Asia*, 2021. 3
- [37] Abhinav Kumar, Garrick Brazil, Enrique Corona, Armin Parchami, and Xiaoming Liu. DEVIANT: Depth EquiVARIANT NeTwork for Monocular 3D Object Detection. In *ECCV*, 2022. 3
- [38] Abhinav Kumar, Garrick Brazil, and Xiaoming Liu. GrooMeD-NMS: Grouped mathematically differentiable nms for monocular 3D object detection. In *CVPR*, 2021. 3
- [39] Trung-Nghia Le, Tam Nguyen, Zhongliang Nie, Minh-Triet Tran, and Akihiro Sugimoto. Anabranh network for camouflaged object segmentation. *CVIU*, 2019. 3, 7, 17
- [40] Aixuan Li, Jing Zhang, Yunqiu Lv, Bowen Liu, Tong Zhang, and Yuchao Dai. Uncertainty-aware joint salient object and camouflaged object detection. In *CVPR*, 2021. 1, 3
- [41] Zeming Li, Chao Peng, Gang Yu, Xiangyu Zhang, Yangdong Deng, and Jian Sun. Light-head R-CNN: In defense of two-stage object detector. *arXiv preprint arXiv:1711.07264*, 2017. 3
- [42] Tsung-Yi Lin, Piotr Dollár, Ross Girshick, Kaiming He, Bharath Hariharan, and Serge Belongie. Feature pyramid networks for object detection. In *CVPR*, 2017. 3, 7
- [43] Tsung-Yi Lin, Priya Goyal, Ross Girshick, Kaiming He, and Piotr Dollár. Focal loss for dense object detection. In *ICCV*, 2017. 1, 3
- [44] Tsung-Yi Lin, Michael Maire, Serge Belongie, James Hays, Pietro Perona, Deva Ramanan, Piotr Dollár, and Lawrence Zitnick. Microsoft COCO: Common objects in context. In *ECCV*, 2014. 7, 17
- [45] Jiannan Liu, Bo Dong, Shuai Wang, Hui Cui, Deng-Ping Fan, Jiquan Ma, and Geng Chen. Covid-19 lung infection segmentation with a novel two-stage cross-domain transfer learning framework. *Medical image analysis*, 2021. 1
- [46] Wei Liu, Dragomir Anguelov, Dumitru Erhan, Christian Szegedy, Scott Reed, Cheng-Yang Fu, and Alexander Berg. SSD: Single shot multibox detector. In *ECCV*, 2016. 1, 3
- [47] Yunqiu Lv, Jing Zhang, Yuchao Dai, Aixuan Li, Bowen Liu, Nick Barnes, and Deng-Ping Fan. Simultaneously localize, segment and rank the camouflaged objects. In *CVPR*, 2021. 3, 7
- [48] Yuxin Mao, Jing Zhang, Zhexiong Wan, Yuchao Dai, Aixuan Li, Yunqiu Lv, Xinyu Tian, Deng-Ping Fan, and Nick Barnes. Transformer transforms salient object detection and camouflaged object detection. *arXiv preprint arXiv:2104.10127*, 2021. 1, 3
- [49] Haiyang Mei, Ge-Peng Ji, Ziqi Wei, Xin Yang, Xiaopeng Wei, and Deng-Ping Fan. Camouflaged object segmentation with distraction mining. In *CVPR*, 2021. 3
- [50] Yuxin Pan, Yiwang Chen, Qiang Fu, Ping Zhang, and Xin Xu. Study on the camouflaged target detection method based on 3D convexity. *Modern Applied Science*, 2011. 1, 3

- [51] Adam Paszke, Sam Gross, Francisco Massa, Adam Lerer, James Bradbury, Gregory Chanan, Trevor Killeen, Zeming Lin, Natalia Gimelshein, Luca Antiga, Alban Desmaison, Andreas Kopf, Edward Yang, Zachary DeVito, Martin Raison, Alykhan Tejani, Sasank Chilamkurthy, Benoit Steiner, Lu Fang, Junjie Bai, and Soumith Chintala. PyTorch: An imperative style, high-performance deep learning library. In *NeurIPS*, 2019. 7
- [52] Joseph Redmon, Santosh Divvala, Ross Girshick, and Ali Farhadi. You only look once: Unified, real-time object detection. In *CVPR*, 2016. 1, 3, 7, 10
- [53] Joseph Redmon and Ali Farhadi. YOLO9000: better, faster, stronger. In *CVPR*, 2017. 1, 3
- [54] Joseph Redmon and Ali Farhadi. YOLOv3: An incremental improvement. *arXiv preprint arXiv:1804.02767*, 2018. 1, 3
- [55] Atique Rehman, Rafia Rahim, Shahroz Nadeem, and Sibt Hussain. End-to-end trained CNN encoder-decoder networks for image steganography. In *ECCVW*, 2018. 6
- [56] Atique-ur Rehman, Rafia Rahim, Shahroz Nadeem, and Sibt-ul Hussain. End-to-end trained CNN encoder-decoder networks for image steganography. In *ECCVW*, 2019. 6
- [57] Jingjing Ren, Xiaowei Hu, Lei Zhu, Xuemiao Xu, Yangyang Xu, Weiming Wang, Zijun Deng, and Pheng-Ann Heng. Deep texture-aware features for camouflaged object detection. *IEEE Transactions on Circuits and Systems for Video Technology*, 2023. 3
- [58] Shaoqing Ren, Kaiming He, Ross Girshick, and Jian Sun. Faster R-CNN: Towards real-time object detection with region proposal networks. *NeurIPS*, 2015. 1, 3, 7, 8, 10
- [59] Nataniel Ruiz, Sarah Adel Bargal, and Stan Sclaroff. Disrupting deepfakes: Adversarial attacks against conditional image translation networks and facial manipulation systems. In *ECCV*, 2020. 1, 2, 3
- [60] Eran Segalis and Eran Galili. OGAN: Disrupting deepfakes with an adversarial attack that survives training. *arXiv preprint arXiv:2006.12247*, 2020. 1, 2, 3
- [61] P Sengottuvelan, Amitabh Wahi, and A Shanmugam. Performance of decamouflaging through exploratory image analysis. In *ICETET*, 2008. 1, 3
- [62] Peize Sun, Rufeng Zhang, Yi Jiang, Tao Kong, Chenfeng Xu, Wei Zhan, Masayoshi Tomizuka, Lei Li, Zehuan Yuan, Changhu Wang, and Ping Luo. Sparse R-CNN: End-to-end object detection with learnable proposals. In *CVPR*, 2021. 7
- [63] Yujia Sun, Geng Chen, Tao Zhou, Yi Zhang, and Nian Liu. Context-aware cross-level fusion network for camouflaged object detection. *arXiv preprint arXiv:2105.12555*, 2021. 1, 3
- [64] Paul Viola and Michael Jones. Rapid object detection using a boosted cascade of simple features. In *CVPR*, 2001. 1
- [65] Paul Viola and Michael Jones. Robust real-time face detection. *IJCV*, 2004. 1
- [66] Chien-Yao Wang, Alexey Bochkovskiy, and Hong-Yuan Liao. YOLOv7: Trainable bag-of-freebies sets new state-of-the-art for real-time object detectors. In *CVPR*, 2023. 3
- [67] Jingdong Wang, Ke Sun, Tianheng Cheng, Borui Jiang, Chaorui Deng, Yang Zhao, Dong Liu, Yadong Mu, Mingkui Tan, Xinggang Wang, Wenyu Liu, and Bin Xiao. Deep high-resolution representation learning for visual recognition. *TPAMI*, 2020. 3
- [68] Run Wang, Felix Juefei-Xu, Meng Luo, Yang Liu, and Lina Wang. FakeTagger: Robust safeguards against deepfake dissemination via provenance tracking. In *ACM Multimedia*, 2021. 1, 2, 3
- [69] Jian-Ru Xue, Jian-Wu Fang, and Pu Zhang. A survey of scene understanding by event reasoning in autonomous driving. *International Journal of Automation and Computing*, 2018. 1
- [70] Fan Yang, Qiang Zhai, Xin Li, Rui Huang, Ao Luo, Hong Cheng, and Deng-Ping Fan. Uncertainty-guided transformer reasoning for camouflaged object detection. In *ICCV*, 2021. 1, 3
- [71] Chin-Yuan Yeh, Hsi-Wen Chen, Shang-Lun Tsai, and Sheng-De Wang. Disrupting image-translation-based deepfake algorithms with adversarial attacks. In *WACVW*, 2020. 3
- [72] Matthew Zeiler and Rob Fergus. Visualizing and understanding convolutional networks. In *ECCV*, 2014. 3
- [73] Qiang Zhai, Xin Li, Fan Yang, Chenglizhao Chen, Hong Cheng, and Deng-Ping Fan. Mutual graph learning for camouflaged object detection. In *CVPR*, 2021. 3
- [74] Xizhou Zhu, Weijie Su, Lewei Lu, Bin Li, Xiaogang Wang, and Jifeng Dai. Deformable DETR: Deformable transformers for end-to-end object detection. In *ICLR*, 2020. 1, 3
- [75] Mingchen Zhuge, Xiankai Lu, Yiyu Guo, Zhihua Cai, and Shuhan Chen. CubeNet: X-shape connection for camouflaged object detection. *Pattern Recognition*, 2022. 3



---

# PrObE: Proactive Object Detection Wrapper

## – Supplementary material –

---

### 1 Proof of Lemma 1

We begin our proof by considering the image  $\mathbf{i}$  as a column vector and the model as a linear regression model with learnable weights  $\mathbf{w}_t$ . The subscript of time  $t$  denotes that the weights change as one performs SGD updates.

**SGD Steps.** We first consider the gradient of weight ( $\mathbf{w}_t$ ). The linear model uses SGD for training, therefore,  $\mathbf{w}_t$  after  $t$  gradient steps is given by:

$$\mathbf{w}_t = \mathbf{w}_0 - \sum_{i=0}^t s_i \mathbf{g}_t = \mathbf{w}_0 - \sum_{i=0}^t s_i \frac{\partial \mathcal{L}}{\partial \mathbf{w}_t}, \quad (1)$$

where, for linear regression model with image  $\mathbf{i}$ ,  $\mathcal{L} = f(\mathbf{w}_t \mathbf{i} - z) = f(\eta)$ . To estimate the gradient  $\mathbf{w}_t$ , we have,

$$\begin{aligned} \mathbf{g}_t &= \frac{\partial \mathcal{L}(\mathbf{w}_t \mathbf{i} - z)}{\partial \mathbf{w}_t} \\ &= \frac{\partial \mathcal{L}(\mathbf{w}_t \mathbf{i} - z)}{\partial (\mathbf{w}_t \mathbf{i} - z)} \frac{\partial (\mathbf{w}_t \mathbf{i} - z)}{\partial \mathbf{w}_t} \\ &= \frac{\partial \mathcal{L}(\eta)}{\partial \eta} \mathbf{i} \\ \mathbf{g}_t &= \mathbf{i}v, \end{aligned} \quad (2)$$

where  $v = \frac{\partial \mathcal{L}(\eta)}{\partial \eta}$  is the gradient of the loss function wrt noise.

**Optimal Weights.** First, we will find the bound of the converged value  $\mathbf{w}_\infty$  and the optimal value  $\mathbf{w}_*$ . If  $\mu_w$  is mean of the learned weight, we have,

$$\begin{aligned} \mathbb{E} \left( \|\mathbf{w}_\infty - \mathbf{w}_*\|_2^2 \right) &= \mathbb{E} \left( \|\mathbf{w}_\infty - \mu_w + \mu_w - \mathbf{w}_*\|_2^2 \right), \\ &= \mathbb{E} \left( (\mathbf{w}_\infty - \mu_w)^T (\mathbf{w}_\infty - \mu_w) \right) + \mathbb{E} \left( (\mu_w - \mathbf{w}_*)^T (\mu_w - \mathbf{w}_*) \right) \\ &\quad + 2\mathbb{E} \left( (\mathbf{w}_\infty - \mu_w)^T (\mu_w - \mathbf{w}_*) \right), \\ &= \mathbb{E} \left( (\mathbf{w}_\infty - \mu_w)^T (\mathbf{w}_\infty - \mu_w) \right) + \mathbb{E} \left( (\mu_w - \mathbf{w}_*)^T (\mu_w - \mathbf{w}_*) \right) \end{aligned} \quad (3)$$

Using  $\mathbb{E}(\mathbf{w}_\infty - \mu_w) = \mathbb{E}(\mathbf{w}_\infty) - \mu_w = \mu_w - \mu_w = 0$ , we have

$$\implies \mathbb{E} \left( \|\mathbf{w}_\infty - \mathbf{w}_*\|_2^2 \right) = \text{Var}(\mathbf{w}_\infty) + \mathbb{E} \left( (\mu_w - \mathbf{w}_*)^T (\mu_w - \mathbf{w}_*) \right) \quad (4)$$

where  $\text{Var}(\mathbf{w}) = \sum_j w_j^2$ .

**Gradient of Weight.** Given the image vector  $\mathbf{i}$ , and noise  $\eta$  are statistically independent, the image and noise gradient  $v$  defined in Eq. (2) are also statistically independent. We also assume that the distribution of image is normal Gaussian ( $\mathbb{E}(\mathbf{i}) = 0$ ). Therefore, the expectation of the gradient  $\mathbf{g}_t$  is given by,

$$\mathbb{E}(\mathbf{g}_t) = \mathbb{E}(\mathbf{i})\mathbb{E}(v) = 0, \quad (5)$$

Next, the variance of  $\mathbf{g}_t$  is given as

$$\text{Var}(\mathbf{g}_t) = \text{Var}(\mathbf{i}v) = \mathbb{E}(\mathbf{i}^T \mathbf{i})[\text{Var}(v) + \mathbb{E}^2(v)] - \mathbb{E}(\mathbf{i})\mathbb{E}(v). \quad (6)$$

We assume that image pixels are normally distributed. This is common since the networks do a mean subtraction before inputting to the network. Thus,  $\mathbb{E}(\mathbf{i}) = 0$ . Hence, we have

$$\text{Var}(\mathbf{g}_t) = \mathbb{E}(\mathbf{i}^T \mathbf{i}) \text{Var}(v). \quad (7)$$

**Converged Weight.** From Eq. (1), the expectation of the weight at time  $t$  is,

$$\begin{aligned} \mathbb{E}(\mathbf{w}_t) &= \mathbb{E}(\mathbf{w}_0) + \sum_{i=0}^t s_i \mathbb{E}(\mathbf{g}_j) \\ &= 0 \text{ (Using Eq. (5))} \end{aligned} \quad (8)$$

Therefore, for converged weight,

$$\begin{aligned} \mathbb{E}(\mathbf{w}_\infty) &= \lim_{t \rightarrow \infty} \mathbb{E}(\mathbf{w}_t), \\ \mathbb{E}(\mathbf{w}_\infty) &= \mathbb{E}(\mu_w) = 0. \end{aligned} \quad (9)$$

For variance, using Eq. (1) we have,

$$\text{Var}(\mathbf{w}_t) = \text{Var}(\mathbf{w}_0) + \left( \sum_i^t s_j^2 \right) \text{Var}(\mathbf{g}_t).$$

Therefore, we have,

$$\begin{aligned} \text{Var}(\mathbf{w}_\infty) &= \lim_{t \rightarrow \infty} (\text{Var}(\mathbf{w}_t)) \\ &= \text{Var}(\mathbf{w}_0) + \left( \lim_{t \rightarrow \infty} \sum_{i=0}^t s_j^2 \right) \text{Var}(\mathbf{g}_t) \\ \text{Var}(\mathbf{w}_\infty) &= \text{Var}(\mathbf{w}_0) + \mathcal{S}' \text{Var}(\mathbf{g}_t). \end{aligned} \quad (10)$$

Substituting Eq. (7) in the above equation, we have

$$\text{Var}(\mathbf{w}_\infty) = \text{Var}(\mathbf{w}_0) + \mathcal{S}' \mathbb{E}(\mathbf{i}^T \mathbf{i}) \text{Var}(v), \quad (11)$$

Going back to Eq. (4), and substituting Eq. (8) and Eq. (10), we have,

$$\begin{aligned} \mathbb{E} \left( \|\mathbf{w}_\infty - \mathbf{w}_*\|_2^2 \right) &= \text{Var}(\mathbf{w}_0) + \mathcal{S}' \mathbb{E}(\mathbf{i}^T \mathbf{i}) \text{Var}(v) + \mathbb{E}(\|\mathbf{w}_*\|_2^2) \\ \implies \mathbb{E} \left( \|\mathbf{w}_\infty - \mathbf{w}_*\|_2^2 \right) &= c + \mathcal{S} \text{Var}(v) \end{aligned} \quad (12)$$

where  $c$  is independent of loss function  $\mathcal{L}$  and  $\mathcal{S} = \mathcal{S}' \mathbb{E}(\mathbf{i}^T \mathbf{i})$  is also another constant.

**Lemma 1.**

We assume that the regression error term  $e = \mathbf{w}^T \mathbf{i} - \hat{y}$ , is drawn from zero mean Gaussian with variance  $\sigma^2$  as in [32]. So,

$$\text{Var}(\hat{e}) = \text{Var}(\mathbf{w}^T \mathbf{i} - \hat{y}) = \sigma^2. \quad (13)$$

For a passive detector with converged weights  $\mathbf{w}_\infty$ , we have,

$$\begin{aligned} \mathbb{E} \left( \|\mathbf{w}_\infty - \mathbf{w}_*\|_2^2 \right) &= c + \mathcal{S} \text{Var}(v) \\ &= c + \mathcal{S} \text{Var}(e) \\ \implies \mathbb{E} \left( \|\mathbf{w}_\infty - \mathbf{w}_*\|_2^2 \right) &= c + \mathcal{S} \sigma^2 \end{aligned} \quad (14)$$

Similarly, for a proactive detector with converged weights  $\mathbf{w}'_\infty$ , we have

$$\mathbb{E} \left( \|\mathbf{w}'_\infty - \mathbf{w}_*\|_2^2 \right) = c + \mathcal{S} \text{Var}(v') \quad (15)$$

Assume that a proactive detector multiplies the input image vector  $\mathbf{i}$  with a scalar template  $s$ . From Eq. (12), we write the loss term as,

$$\begin{aligned}\mathcal{L}' &= \frac{1}{2} (s\mathbf{w}^T \mathbf{i} - \hat{y})^2 \\ \implies \frac{\partial \mathcal{L}'}{\partial \mathbf{w}} &= (s\mathbf{w}^T \mathbf{i} - \hat{y})s\mathbf{i}\end{aligned}\quad (16)$$

Taking the variance,

$$\begin{aligned}\text{Var}(v') &= \text{Var}\left(\frac{\partial \mathcal{L}'}{\partial \mathbf{w}}\right) = \text{Var}((s\mathbf{w}^T \mathbf{i} - \hat{y})s\mathbf{i}) \\ &= \text{Var}(s(\hat{y} + e) - \hat{y})s^2 \text{Var}(\mathbf{i}) \quad , \text{ assuming } \mathbb{E}(\mathbf{i}) = 0 \\ &= \text{Var}(se + (s-1)\hat{y})s^2 \text{Var}(\mathbf{i}) \\ &= (\text{Var}(se) + \text{Var}((s-1)\hat{y}))s^2 \text{Var}(\mathbf{i}) \\ &= s^2 \text{Var}(e)s^2 \text{Var}(\mathbf{i}) \quad , \text{ assuming } \text{Var}(\hat{y}) = 0 \\ &\leq s^2 \text{Var}(e)s^2 \quad , \text{ assuming } \text{Var}(\mathbf{i}) \leq 0.5 \times (-1)^2 + 0.5 \times 1^2 = 1 \quad (17) \\ \implies \text{Var}(v') &\leq s^4 \sigma^2 \quad (18)\end{aligned}$$

If the magnitude of the scalar template is bounded by 1 i.e.,  $s^2 < 1$ , we have

$$\text{Var}(v') < \sigma^2. \quad (19)$$

The above shows that the gradients in the proactive model has less noise than the passive model (a key for better convergence). Substituting above in Eq. (15), we have

$$\begin{aligned}\mathbb{E}\left(\|\mathbf{w}'_\infty - \mathbf{w}_*\|_2^2\right) &= c + \mathcal{S}\text{Var}(v') \\ &< c + \mathcal{S}\sigma^2 \\ &< c + \mathcal{S}\text{Var}(v) \\ \implies \mathbb{E}\left(\|\mathbf{w}'_\infty - \mathbf{w}_*\|_2^2\right) &< \mathbb{E}\left(\|\mathbf{w}_\infty - \mathbf{w}_*\|_2^2\right).\end{aligned}\quad (20)$$

The last inequality follows trivially from Eq. (14).

## 2 Proof of Theorem 1

From Lemma 1, we have,

$$\begin{aligned}\mathbb{E}\left(\|\mathbf{w}'_\infty - \mathbf{w}_*\|_2^2\right) &< \mathbb{E}\left(\|\mathbf{w}_\infty - \mathbf{w}_*\|_2^2\right) \\ \implies \text{Var}(\mathbf{w}'_\infty) &< \text{Var}(\mathbf{w}_\infty) \\ \implies \mathbb{E}(|\mathbf{w}'_\infty{}^T \mathbf{i} - y|) &< \mathbb{E}(|\mathbf{w}_\infty{}^T \mathbf{i} - y|) \\ \implies \mathbb{E}(\hat{y}' - y) &< \mathbb{E}(\hat{y} - y)\end{aligned}\quad (21)$$

Since the proactive detector has a better bounding box prediction,

$$\implies \mathbb{E}(\text{IoU}'_{2D}) > \mathbb{E}(\text{IoU}_{2D}) \quad (22)$$

Since  $AP$  is a non-decreasing function of  $\text{IoU}_{2D}$ , we have,

$$AP' \geq AP. \quad (23)$$

An important point to note is that the non-decreasing nature does not keep the inequality strict. In other words, we agree that the final AP from passive and pro-active schemes could be equal. However, our experience says that IoU improvements, especially close to 1, lead to significant AP improvements. Current SoTA detectors already achieve decent IoU; hence, even a slight improvement in IoU improves the AP score.

**Table 1: Ablation of training iterations** on DGNet for more iterations similar to after applying PrObE D.

Method	Iter	$E_m \uparrow$ $S_m \uparrow$ $wF_\beta \uparrow$ $MAE \downarrow$				$E_m \uparrow$ $S_m \uparrow$ $wF_\beta \uparrow$ $MAE \downarrow$				$E_m \uparrow$ $S_m \uparrow$ $wF_\beta \uparrow$ $MAE \downarrow$			
		CAMO				COD10K				NC4K			
DGNet [34]	1×	0.859	0.791	0.681	0.079	0.833	0.776	0.603	0.046	0.876	0.815	0.710	0.059
DGNet [34]	2×	0.861	0.791	0.682	0.080	0.832	0.778	0.606	0.045	0.875	0.814	0.711	0.059
+ PrObE D	2×	<b>0.871</b>	<b>0.797</b>	<b>0.702</b>	<b>0.071</b>	<b>0.869</b>	<b>0.803</b>	<b>0.661</b>	<b>0.037</b>	<b>0.900</b>	<b>0.838</b>	<b>0.755</b>	<b>0.049</b>

**Table 2: Ablation of dice loss with cross-entropy (CE) loss vs. cosine similarity**

Method	CAMO				COD10K				NC4K			
	$E_m \uparrow$	$S_m \uparrow$	$wF_\beta \uparrow$	$MAE \downarrow$	$E_m \uparrow$	$S_m \uparrow$	$wF_\beta \uparrow$	$MAE \downarrow$	$E_m \uparrow$	$S_m \uparrow$	$wF_\beta \uparrow$	$MAE \downarrow$
Dice + CE loss	0.831	0.782	0.688	0.084	0.810	0.795	0.646	0.045	0.874	0.817	0.721	0.060
Cosine similarity	<b>0.871</b>	<b>0.797</b>	<b>0.702</b>	<b>0.071</b>	<b>0.869</b>	<b>0.803</b>	<b>0.661</b>	<b>0.037</b>	<b>0.900</b>	<b>0.838</b>	<b>0.755</b>	<b>0.049</b>

### 3 Implementation Details

We now include more details of our method here.

**Network Architecture.** The network architecture of encoder  $\mathcal{E}$  and decoder  $\mathcal{D}$  network used for PrObE D is shown in Fig. 1. Both networks consist of 2 stem convolution layers and 13 blocks, each block containing convolutional, batch normalization, and ReLU activation layers. The images are given as input to the encoder network to output the template, which is multiplied by the input images to make them encrypted. The encrypted images are then passed to the decoder network to recover the template. Finally, we input encrypted images to different object detectors to perform detection.

**Dataset license information.** We use benchmark datasets for GOD and COD. The authors for MS-COCO [44] dataset specify that the annotations in this dataset, along with this website, belong to the COCO Consortium and are licensed under a Creative Commons Attribution 4.0 License. The COD10K dataset is available for non-commercial purposes only [17]. The CAMO data is published under the Creative Commons Attribution-NonCommercial-ShareAlike 3.0 License [39]. Finally, the NC4K dataset is available to use for non-commercial purposes.

**Experimental Setup and Hyperparameters.** PrObE D is trained in an end-to-end manner for all the object detectors, with training iterations similar to the pretrained object detector. For both encoder and decoder networks, we use Adam optimizer with a learning rate of  $1e^{-5}$ . We use different weights of  $[\lambda_{OBJ}, \lambda_E, \lambda_D]$  for different object detectors. We use [7,10,10] for Faster-RCNN, [50, 1.25, 4.25] for YOLOv5, [50, 7.5, 7.5] for DeTR and [10, 0.1, 0.1] for DGNet. All experiments are conducted on one NVIDIA A100 GPU.

### 4 Additional Experiments

**Train COD detector DGNet more.** Similar to the GOD detector, we train the COD detector DGNet for more iterations, similar to after applying PrObE D. The results are shown in Tab. 1. We see a similar behavior as seen in GOD detectors; the performance improves after training for more iterations, but only up to a certain extent. PrObE D is able to improve performance by a larger margin, showing the effectiveness of the proactive schemes.

**COD loss.** Our loss design is inspired by the prior proactive works [1, 2], which estimate the learnable template by applying a cosine similarity loss. The authors experiment with various loss types, showing the effectiveness of the cosine similarity loss design. However, COD is analogous to the segmentation task, which generally adopts a loss design of cross-entropy loss with dice loss, which might be beneficial for COD. We perform an ablation by applying cross-entropy loss with dice loss for COD. The results are shown in Table 2. We see that our proactive wrapper is not benefiting by removing the cosine similarity loss, proving the study of the prior proactive works.

**Error analysis.** Following [6], there can be a number of errors that deteriorate the performance of the object detector. These are:

1. Classification error (Cls): Localized correctly but classified incorrectly.
2. Localization error (Loc): Classified correctly but localized incorrectly.

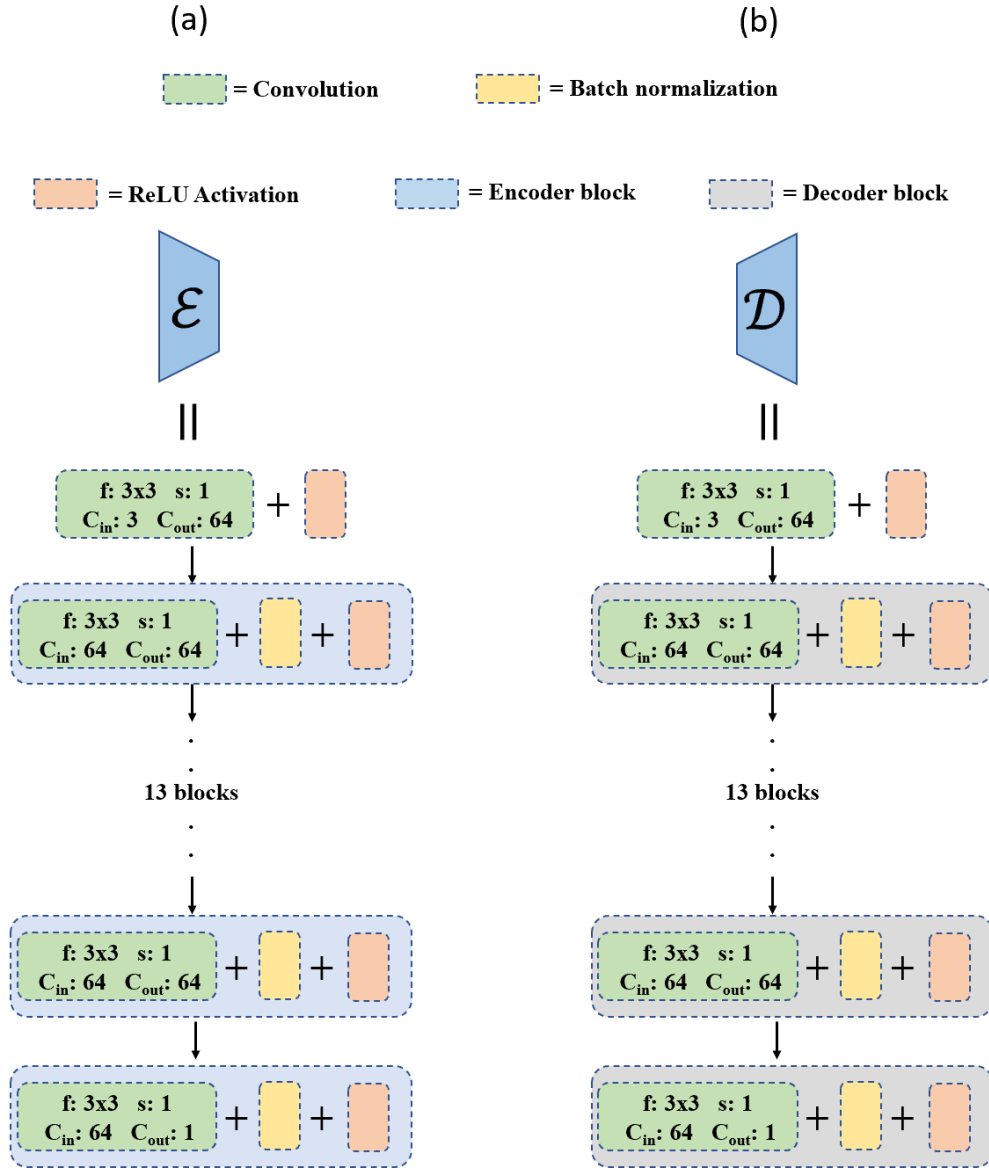
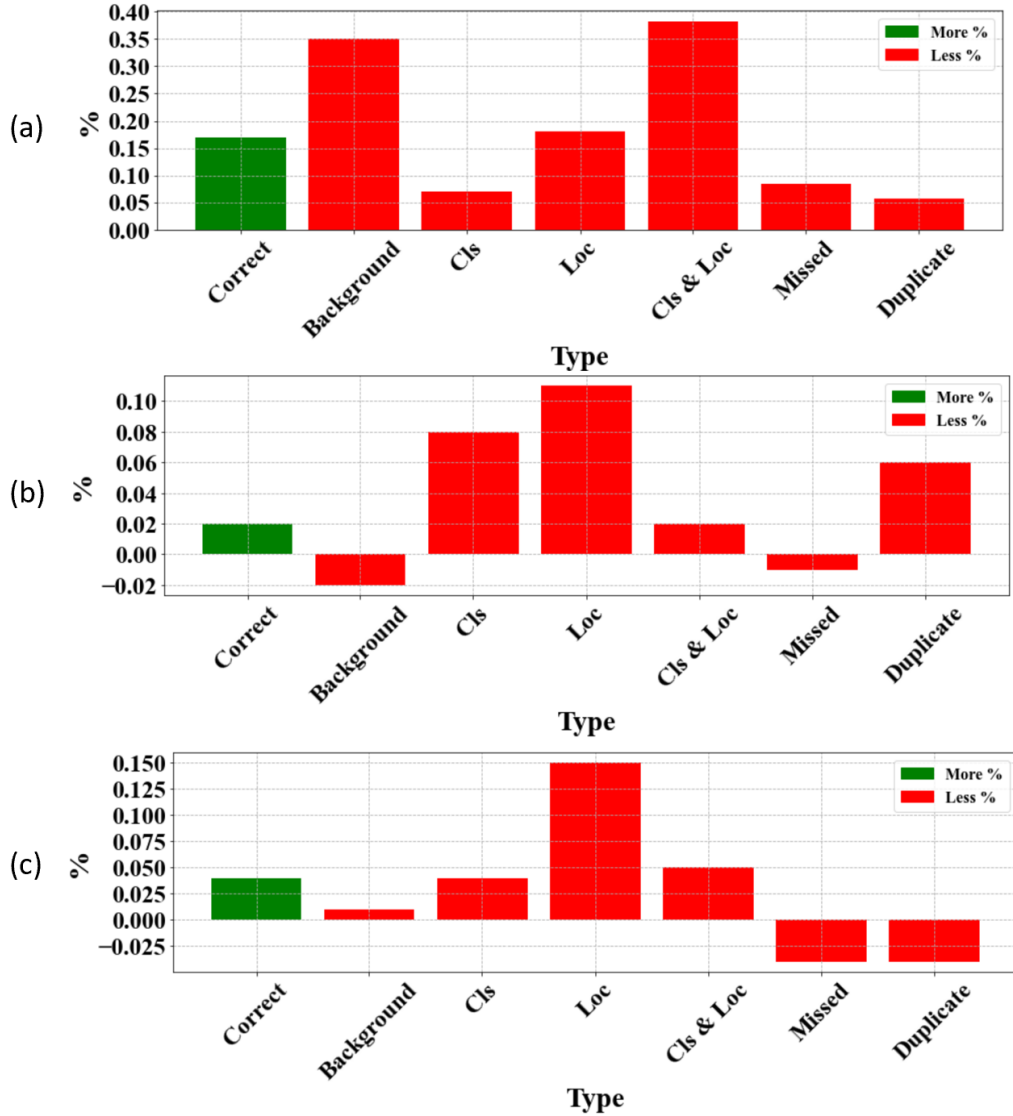


Figure 1: Architecture for encoder and decoder network.

3. Both Classification and Localization error (Cls & Loc): Classified and localized incorrectly.
4. Duplicate detection error (Duplicate): Would be correct if not for a higher scoring detection.
5. Background error (Background): Detected background as foreground.
6. Missed target error (Missed): All undetected targets *i.e.* false negatives, which are not already covered by classification or localization errors.

Fig. 2 shows the error analysis for three object detectors, namely, Faster-RCNN, YOLOv5, and DeTR. PrObE improves the number of correct predictions of all three detectors, especially for Faster-RCNN, where the number of correct predictions increases by around 17%. For DeTR and YOLOv5, the improvement is less, which is evident from the less increase in correct predictions. The major improvement for all three detectors comes from classification and localization-related errors. All these errors decrease after PrObE is applied to all the detectors. Further, Faster-RCNN, being an old detector, makes a lot of background errors, which are reduced by a significant margin





**Figure 2: Error analysis** for (a) Faster-RCNN, (b) YOLOv5, and (c) DeTR. PrObE is able to improve the number of correct predictions and reduce most errors.

after applying PrObE. The gain is not much for DeTR and YOLOv5, which tend to make fewer background errors. Finally, one-stage detectors suffer mostly from the problem of duplicate detection, which is remedied by the PrObE.

## 5 Potential Negative Societal Impact

PrObE utilizes a proactive scheme to benefit object detection. Our approach can be considered a benign adversarial attack on object detectors. However, with a change in the objective function, PrObE could also be used as an adversarial attack to deteriorate the performance of different object detectors. This might pose a threat to object detectors, whether used for GOD or COD, and some forms of adversarial training might be required to prevent the threat of adversarial attacks.